5-2019

Gas Chromatography Analysis of CO2 Reduction Photocatalysis with Zinc Dipyrrin Complexes

Alex Day

Gas Chromatography Analysis of CO_2 Reduction Photocatalysis with Zinc Dipyrrin Complexes

_____

A thesis

presented to

the faculty of the Department of Chemistry

East Tennessee State University

In partial fulfillment

of the requirements for the

University Honors Scholar Program

_____

by

Alex Day

April 2019

_____

Thesis Advisor: Dr. McCusker _____

2nd Reader: Dr. Scott _____

Keywords: GC (gas chromatography), CO_2 Reduction, Photocatalysis, ZnDPY, Dipyrrin

ABSTRACT

Gas Chromatography Analysis of CO_2 Reduction Photocatalysis with Zinc Dipyrrin Complexes

by

Alex Day

Bis(1,3,7,9-tetramethyl-5-mesityldipyrrinato)zinc(II) (ZnDPY) was synthesized in the lab by the McCusker group and a procedure was created to analyze its ability as a photosensitizer, a molecule that provides the energy for the reaction to occur by capturing light energy and turning it into a form that can be used by the photocatalyst. While more work is needed, preliminary steps have been made to create a process that can analyze the amount of carbon monoxide produced by a photocatalytic CO_2 reduction reaction with ZnDPY as the photosensitizer. Progress has been made via the setup of a reaction apparatus, targeted gas chromatography (GC) peak separation, and GC calibration. More work will need to be done in order to determine the optimal reaction mix to showcase the sensitizer's potential.

ACKNOWLEDGMENTS

I would like to thank my research adviser Dr. McCusker, who helped me whether it be in the classroom or in the lab and pushed me to improve as a student. I would also like to thank my second reader, Dr. Scott, who provided insights on the analytical chemistry components of the research project. Lastly, I would like to thank my lab partner Senan, whom I worked with to make this project happen and provided the numbers for all the reduction potentials.

I offer a big thanks to the organizations that made this work a reality. I would like to thank the Honors College of ETSU, who accepted me into their program and provided for my education up to this point. None of this would have happened if I were not a part of this program, and it is because of them that I had such a wonderful college experience here at ETSU. Lastly, I would like to thank the ETSU's Office of Research and Sponsored Programs Administration and the American Chemical Society's Petroleum Research Fund. Both of these programs funded this project. I appreciate them for providing the McCusker research group the means to perform our projects.

TABLE OF CONTENTS

Page

LIST OF TABLES AND FIGURES

LIST OF ABBREVIATIONS

Abbreviation	Name
GC	Gas Chromatography
ZnDPY	Bis(1,3,7,9-tetramethyl-5-mesityldipyrrinato)zinc(II).
BODIPY	4,4-difluoro-4-bora-3a,4a-diaza-s-indacene
FeF20TPPCl	5,10,15,20-Tetrakis(pentafluorophenyl)-21H,23H-porphyriniron(III) chloride
THF	Tetrahydrofuran
TCD	Thermal Conductivity Detector

INTRODUCTION

The Role of CO_2

The carbon cycle is an important feature in the biosphere of our world. Many organisms produce CO_2 as an end-product of their metabolism, which is cycled back into organic matter by other organisms and other natural processes. Like many things in nature, there is an important balance that needs to be maintained to properly facilitate life. For the past several decades, there has been evidence that this balance is starting to falter. The current trend is that the earth has been getting increasingly warm at an unprecedented rate. The past two National Climate Assessments have shown results similar to the models of predicted climate change with 2012 being the hottest year on record since the early 1900's.[1] The general trend holding true, the current top 5 warmest years on record occurred within the last 5 years from 2018.[2] This change in climate has led to reduced polar ice caps, more severe weather, and increased numbers of extinction among other detriments.[1, 3-4]

Even with this threat, dealing with climate change is a complex issue due to the socioeconomic issues that underlie it. The modern world is heavily dependent on fossil fuels, which in turn produce most of the greenhouse gases that are credited for the drastic rate of temperature increase.[5-6] While one of the best methods to mitigate and even reverse climate change would be to change our habits, there are many who have no interest in doing so and others who do not believe that it is caused by humanity. Finding ways to remove greenhouse gases from the atmosphere is normally a popular option, but there are concerns that drastically implementing just a single method will not be enough, no matter how popular.[7]

When it comes to a situation with no silver bullet, it is often helpful to amass as many useful tools in which to tackle the problem as possible. One of the most promising in the chemistry field is CO_2 reduction photocatalysis, a method beautiful in its efficiency. While there are numerous greenhouse

gases and several more potent than CO_2,[8] CO_2 is often the target of many sustainability efforts, likely due to its presence in the stages of the carbon cycle as well as its prevalence in general.[9] CO_2 is the main greenhouse gas emitted by humans, comprising 81.6 % of greenhouse gases created in the U.S. in 2016.[8] While this is by no means the only solution toward reducing CO_2,[10] the beauty of CO_2 reduction photocatalysis is that it does so by using the renewable energy of the sun to turn it into useful products. Promising as it may be, there is much work to be done to make this a viable tool to mitigate the effects of climate change.

Converting CO_2 into even something like methane is no small task. Synthesizing this would involve 8 electrons and 818 kJ/mol.[11] Indeed, the most common gaseous products of CO_2 reduction efforts are methane and CO while methanol is common in the liquid phase.[12] The methods of CO_2 reduction, however, have seen much more diversity. Carbon dioxide reduction has ranged from manipulating the biological methods of organisms to synthesize desired products to developing a wide range of different catalysts to integrating electrochemistry into the systems.[11] This project focuses on analyzing the results of a reaction with bis(1,3,7,9-tetramethyl-5-mesityldipyrrinato)zinc(II) (ZnDPY) (Figure 1) and 5,10,15,20-tetrakis(pentafluorophenyl)-21H,23H-porphyriniron(III) chloride (FeF20TPPCl), a known catalyst deemed appropriate to work with ZnDPY to reduce CO_2 through a comparison of voltage potentials.

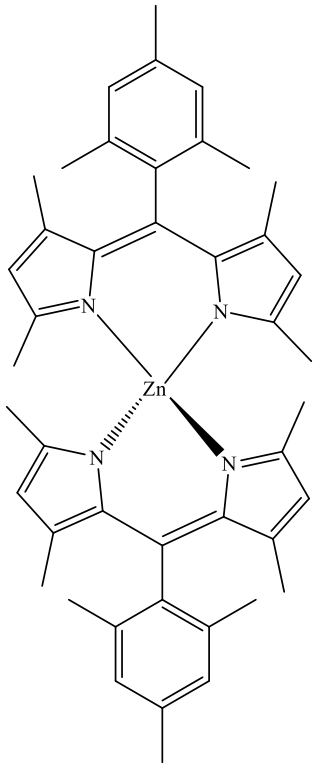

Figure 1. Chemical structure of bis(1,3,7,9-tetramethyl-5-mesityldipyrrinato)zinc(II) (ZnDPY).

Relevant Photocatalysis Mechanisms

Before explaining the significance of ZnDPY, it is best to discuss the operation of a photocatalysis reaction. In any given photocatalysis reaction, several roles must be filled for it to take place. While there are cases of molecules taking on several of these roles in photocatalysis,[13] in this experiment's setup, a photosensitizer captures the energy from the light, a sacrificial electron donor supplies the electrons, and a photocatalyst catalyzes a reaction. This setup allows different components of the photocatalytic reaction to be varied and the resulting effects to be tested. In particular, this means having the ability compare the effectiveness of the photosensitizer with different photocatalysts.

There are two quenching pathways in which CO_2 can be reduced. Figure 2a shows the oxidative quenching pathway and Figure 2b shows the reductive quenching pathway. In the oxidative pathway, a photon of light (hv) is absorbed by the photosensitizer (S) and transitions into an excited state (S*). The excited state is then able to reduce the photocatalyst (Cat). Afterward, the electron donor (D) donates

an electron to regenerate the oxidized photosensitizer ($S^+ \rightarrow S$). In the second pathway, a photon of light (hv) is absorbed by the photosensitizer (S) and the molecule transitions into an excited state, (S*). The electron donor (D) then reduces the excited photosensitizer, resulting in a reduced photosensitizer (S^-). The reduced photosensitizer then reduces the photocatalyst (Cat) and is left ready to start the cycle again. While both mechanisms are possibilities, it is important to note that the pathway can be limited by the choices of the components (see paragraph under Figure 7).

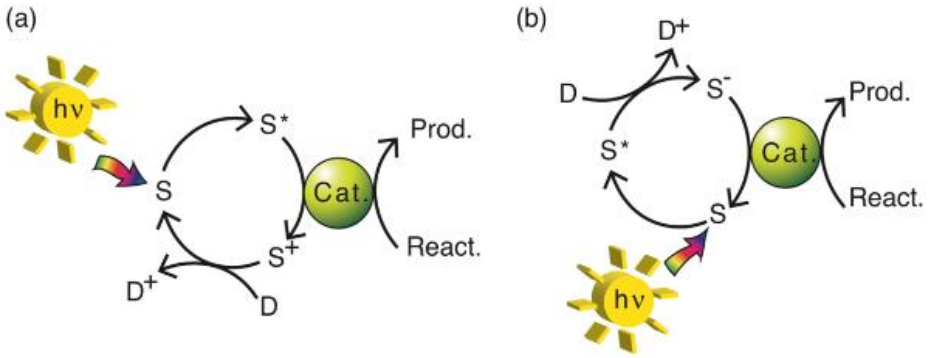

Figure 2. Oxidative (a) and reductive (b) quenching pathways for reductive photocatalysis. hv represents the photon, S represents the sensitizer, D represents the electron donor, and Cat represents the catalyst. The arrow that points from React. to Prod. represent the catalysis reaction taking place.[14]

Assigning the roles of the photosensitizer and photocatalyst to different molecules allows one to vary the photosensitizer and the photocatalyst to perform a systematic array of experiments but this experimental flexibility comes with a cost. The photosensitizer must maintain an excited state long enough for it to diffuse through the solution to reach a photocatalyst molecule. A triplet excited state would allow the molecule to maintain sufficient energy long enough to be utilized by the reaction due to the involvement of a spin-forbidden transition, when an electron flips its spin during transition. These transitions take place as the molecule relaxes from the triplet excited state to the ground state and take a long time to occur due to the low probability of an electron changing its spin over time. Photosensitizers that can produce this excited state are sought after for these types of reactions.

Relevant Electron Excited States

When a photon of sufficient energy excites a molecule, it has the ability to move to a higher energy state through a process called absorption. Figure 3 shows this process as well as several of the processes that could happen after absorption of that energy. The two most important for this discussion are fluorescence and phosphorescence. Fluorescence occurs when a molecule transitions back to the ground state from a singlet excited state. Phosphorescence occurs from the radiative decay of a triplet excited state to the ground state. In order for this to occur, a transition from one spin multiplicity to another in which a singlet state transitions to a triplet state and vice versa take place by flipping the spin of an electron. The process of changing spin multiplicities requires considerably more time than just the radiative decay between two states of the same spin multiplicities, which causes the emission of energy through phosphorescence to take more time. Phosphorescence thus takes considerably longer than normal fluorescence to occur and is associated with the formation of a triplet state. Important to note, however, is that molecules can be excited into a triplet excited state without phosphorescing, as is the case with ZnDPY at room temperature. The triplet state can still be detected through other means such as transient absorption spectroscopy. [14]

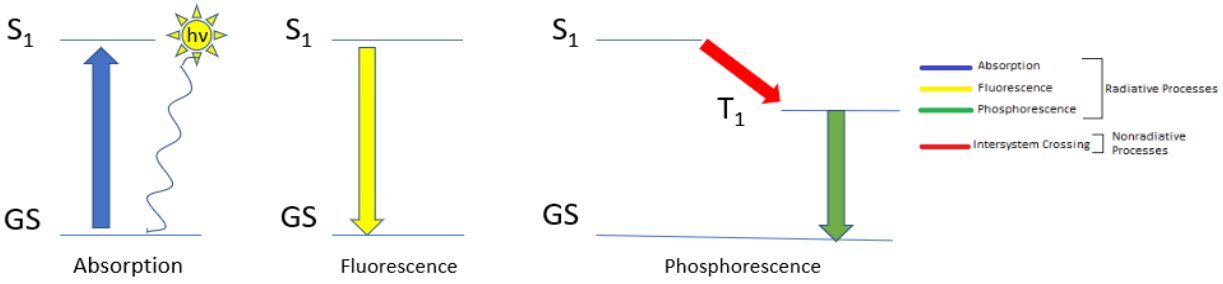

Figure 3. Jablonski diagram, showing energy transitions that result in fluorescence and phosphorescence. S_1 represents the singlet excited state, GS represents the singlet ground state, and T_1 represents the triplet excited state. The arrows represent the transition from one state to the state the arrow points to according to the color key. The wavy line with the image of a sun represents the stream of photons from a light source.

Why Zinc Dipyrrin Dyes?

Zinc dipyrrin dyes were chosen by the McCusker group for a number of reasons including the ability to produce these long-lived triplet states.[15-16] Zinc dipyrrin dyes have been widely explored for their electrochemical and photochemical properties,[15, 17-19] but no papers were found regarding their use as photosensitizers. This makes photocatalytic research using zinc dipyrrin dyes an exciting new study. Complexes with dipyrrin ligands (Figure 4) have become interesting molecules of study in this field of work due to their high luminescent quantum yields and tunable emission properties.[19-22] Zinc dipyrrin dyes are of interest due to their similarities to 4,4-difluoro-4-bora-3a,4a-diaza-s-indacene (BODIPY) dyes without some of their poor qualities as photosensitizers.[14] BODIPY dyes (Figure 5) have been shown to have a very high fluoresce quantum yield. This means that most of the energy the molecule absorbs is emitted via the process of fluorescence, leaving little room for other processes that involve longer-lived excited states to occur. While zinc dipyrrin dyes are not able to phosphoresce at room temperature, they are able to form triplet excited states increasingly with the polarity of the solvent.[14]

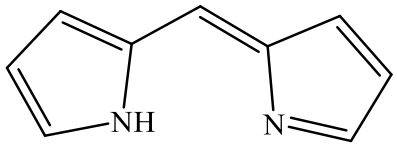

Figure 4. Chemical structure of the dipyrrin ligand, which can be modified and attached to different metals.

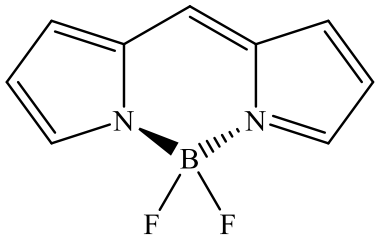

Figure 5. Chemical structure of the BODIPY core.

One of the processes that can occur in dipyrrin complexes with two dipyrrin ligands is the formation of a charge separated state, where one ligand is oxidized and the other is reduced. Polar

solvents help stabilize this state, lowering its energy and make making the conversion from a singlet excited state to a charge separated state more favorable. This state is theorized to lead to the formation of triplet excited states and is a potential cause of the formation of a triplet excited state in ZnDPY. Furthermore, their structure lends itself to absorbing more solar radiation than BODIPY dyes due to the presence of a second dipyrrin ligand. An issue with many current photosensitizers is that many of them are made of rare metals and are thus more expensive to synthesize. On top of potentially being part of useful photosensitizers, zinc is more common and thus less expensive, making the photosensitizer that utilizes it more commercially viable.[14]

Other Components of the Reaction

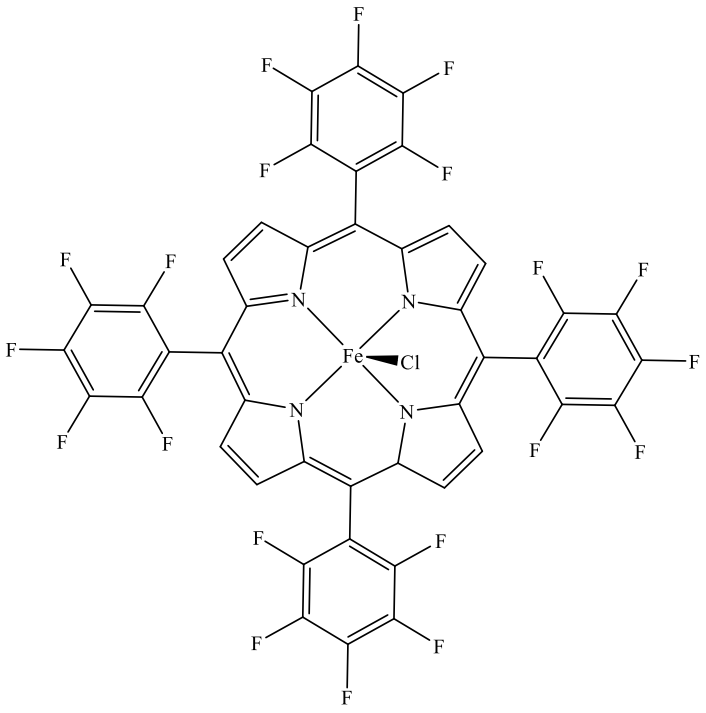

Figure 6. Chemical structure of 5,10,15,20-tetrakis(pentafluorophenyl)-21H,23H-porphyriniron(III) chloride (FeF20TPPCl)

In order for the photocatalysis reaction to proceed, an appropriate catalyst must be paired with the photosensitizer. An appropriate catalyst is one that can be reduced by the photosensitizer. The catalyst has a reduction potential of -1.362 V vs. SCE [23]. This is higher than the reduction potential of the photosensitizer (-1.782 V vs. SCE) and can thus be reduced by it. Furthermore, there are examples of

iron tetraphenylporphyrin complexes being used in both electrocatalytic[24-25] and photocatalytic CO_2 reduction processes.[26-27] Given its commercial availability on top of all these other factors, FeF20TPPCl was chosen.

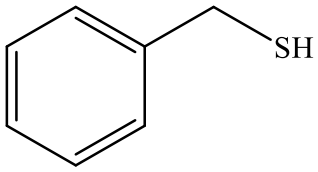

Figure 7. Chemical structure of benzyl mercaptan.

Benzyl mercaptan (Figure 7) was chosen as the electron donor used in the experiment to test the abilities of the photosensitizer. This electron donor has the ability to reduce the excited ZnDPY molecule since the electron donor has an oxidation potential of -0.1 V vs. SCE[28] and the excited ZnDPY molecule has a reduction potential of -0.042 V vs. SCE. With the current choices of electron donor and catalyst, only one of the quenching pathways can occur. Once the photosensitizer is excited by the light, the electron donor can fill the electron hole left from the transition of an electron from highest occupied molecular orbital to the lowest occupied molecular orbital. This process causes the excited ZnDPY molecule to transition into the molecule's reduced state, which has a reduction potential high enough (-1.782 V vs. SCE) to reduce the iron catalyst. In order for the oxidative quenching pathway to occur, the excited state of the photosensitizer would have to be able to reduce the iron catalyst. This is not possible given the excited state has an oxidation potential of -0.803 V vs. SCE and the iron catalyst has a reduction potential of -1.362 V vs. SCE.[23] Given that converting CO_2 to CO has a reduction potential of -0.771 V vs SCE,[14] the catalyst can reduce CO_2 to CO because of its higher reduction potential.

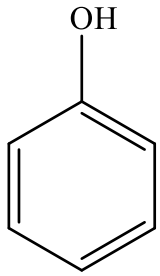

Figure 8. Chemical structure of phenol.

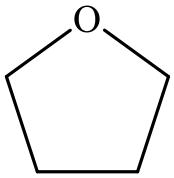

Figure 9. Chemical structure of tetrahydrofuran

Phenol was a component used in the initial experiments as an acid synergist. It has been found that these synergists help stabilize the $Fe^{II}CO_2^{2-}$ complex by hydrogen bonding. This stabilizes an intermediate in the CO_2 reduction reaction and assists in directing electrons out of the substrate (CO_2) as the catalyst directs electrons into the substrate.[29] Furthermore, this chemical serves as a cosubstrate, contributing H^+ atoms to the reaction.[23] All of the chemicals in the reaction mix are soluble in tetrahydrofuran (THF) and so it was used as a solvent.

GC Information

Gas chromatography is a useful tool to analyze the components of a volatile sample. It is a very flexible method to quantify the components of a sample, but that leaves several variables to consider. One of the ultimate goals of gas chromatography is to attain efficient peak separation so that one can easily use the peak area to quantify the amount of the components in the sample based on prior calibration. The carrier gas, column type, flow rate, and oven temperature are parameters that can affect the separation of a sample and must be optimized.

Columns come in many different types and sizes and separate gases based on several factors. Columns separate gases based on size, polarity, and other chemical properties. Column length can be varied to increase and decrease retention time, but this may come at the cost of longer and shorter run times respectively. Columns must be prepared before they can be used by the GC. Unlike most other variables, the column usually takes more maintenance. There is often an installation process and maintenance is required periodically.

The oven temperature helps separate the components in a run by changing the speed in which they elute. Gases will have more kinetic energy to move through the column with increasing temperature, a property that can be particularly useful for gases that adhere well with the column. The oven temperature program can be varied in several ways to facilitate the controlled separation of the components. Not only can the temperature be changed from run to run, the temperature can also be varied at different times throughout the run to optimize separation. Higher oven temperatures can decrease retention time, but at the sacrifice of peak separation. Lower oven temperatures can result in better separation if done correctly but can also result in wider peaks.

The role of the carrier gas is self-explanatory in that it carries the sample gas through the instrument, but it plays a role in the type of settings that one must use in order to conduct successful runs. Common carrier gases include helium, hydrogen, and nitrogen.[30-31] While any of the high-purity versions of these gases would work, adjusting other separation variables are important to yield adequate separation. While choice of carrier gas is important, the rate at which it flows is also important. The carrier gas can also factor into what flow rate should be used,[30] and the flow rate can be increased or decreased to affect retention time.

MATERIALS AND METHODS

Gas Chromatography Setup

The GC used in this experiment was Model 333 from SRI Instruments connected to a computer with Peak454 software. For the purposes of this experiment, carbon dioxide and carbon monoxide are the main considerations concerning the detection of products for the photochemical reaction. A thermal conductivity detector (TCD) from SRI Instruments was chosen due to its ability to detect the gases expected to be produced by the experiment.[32] A TCD analyzes a sample by comparing the difference between the thermal conductivity of the carrier gas and the sample. A 5 Å molecular sieve column was utilized for its ability to separate small molecules based on size. Molecules smaller than 5 angstroms pass through the column, allowing hydrogen, oxygen, and carbon monoxide to produce peaks. Carbon dioxide is known to get stuck in the pores due to its size and is a concern because it can block the path for the other smaller sample gases.[33] Carbon dioxide can be released from the column with the appropriate drying procedure, which is outlined by reference 34.

Calibration

The first step in calibrating the instrument was to obtain optimal peak separation. This was attained using different experiments with Scott Mini-Mix calibration gas (0.5% by mol CO_2, CO, O_2, and H_2 in nitrogen gas) in which the column temperature and flow rate were varied. These experiments were preceded by a procedure to zero the TCD, which was conducted to account for any background noise that was detected by the instrument. This was done by releasing the ultrapure nitrogen carrier gas through a nozzle, turning on the TCD, setting the oven temperature to 80°C, setting the TCD cell to 205°C, and letting the program run for 7 minutes before activating the option to zero the detector. The parameters for this procedure was created from a combination of the TCD cell temperature (205°C) used in the experiment and instructions taken from the manual to check and zero the detector.[35] From there, a number of trials were conducted in order to find the best separation method. While the column

and TCD cell temperature remained constant, the carrier gas flow rate and the oven temperature (or column temperature) were varied in order to yield the best results. Ideally, this would mean relatively narrow, distinguishable peaks representing the gases that may be produced by the reduction reaction.

Once adequate peak separation was achieved, peaks from the calibration gas GC runs were assigned so that calibration could proceed. Because every gas interacts with a given column in a particular way, gases will elute in a particular order based on the strength of that interaction. This allowed the identity of the peaks to be determined by comparison to a literature source from the manufacturer of the column and process of elimination. Known amounts of calibration gas were injected to make a calibration curve. This curve relates the amount of gas detected by corresponding that amount to a peak area given by the GC. Nine samples of Scott Mini-Mix sample gas (0.5% by mol CO_2, CO, H_2, and O_2 respectively in nitrogen) were taken through a 1 mL gas-tight syringe from a regulator attached to the cylinder and injected in increasing 0.1 mL increments to produce a linear calibration curve. Using the ideal gas law equation (1), the volume amounts were converted into mole amounts of gas injected, namely that for CO. Equation (2) denotes an example with a pressure of 1 atm, a volume of 0.001 L, a room temperature of 293.65 K, and the appropriate ideal gas constant. Equation (2) rearranges equation (1) algebraically to solve for n, the number of moles.

$$PV=nRT \qquad (1)$$

$$n= (1\ atm)(0.001\ L)/((0.082057\ L\ atm\ mol^{-1}K^{-1})(293.65\ K))= 4.15x10^{-5}\ moles \qquad (2)$$

Because the nitrogen carrier gas was used instead of helium, negative peak values were produced. Thermal conductivity detectors work by comparing the difference between the carrier gas and the carrier gas with the sample, and the TCDs of many GCs often come programmed for helium. Since all the gases have a lower conductivity compared to helium, the peaks are negative. As a default setting, the software also produced many blue integration lines that cluttered the graph (see Figure 10).

To rectify this, the reverse integration peak function in the peak simple software was utilized in order to produce more familiar graphs, and the integrate field was unchecked on the channel menu.

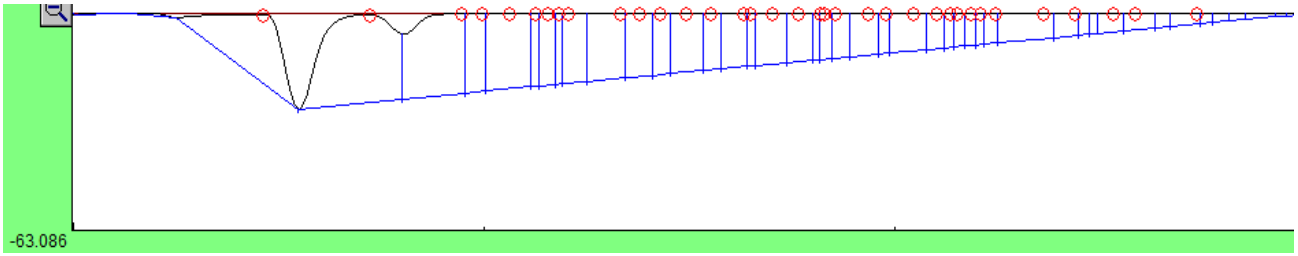

Figure 10. Graph of a 0.5 mL injection of calibration gas with an oven temperature of 70°C and a flow rate of 15 mL/min with default settings.

Reaction Setup

Tests were conducted to determine what would be necessary in the reaction apparatus that would test ZnDPY. One of these experiments involved testing different submersible water pumps to see if they could be configured to match the flow rate of the Fisher Science Isotemp 4100 R20F refrigerating/heating bath circulator (circulator). A tygon hose carrying water from the circulator was set in a container which housed a submersible water pump. The pump was then connected back to the circulator, and water flow was adjusted between the container and the circulator to best facilitate an equal rate of water flow. Since the circulator could not have its flow rate adjusted, the water pumps were adjusted in attempt to match the input and output of water long enough to facilitate a temperature controlled photocatalysis reaction with ZnDPY.

Another set of experiments involved assessing whether the circulator would be enough to keep the temperature relatively constant on its own. A 300 W Xe Arc lamp from Oriel Instruments, model 66901 was set to 275 W by a power supply from Oriel Instruments, model 69911 and directly illuminated a water jacketed reaction flask (photoreactor) set to a constant temperature via the circulator. A given temperature was set on the circulator and this was compared to the temperature of the water (measured by mercury thermometer) in the photoreactor that was placed under temperature control.

Research toward creating an optimized reaction method is still underway, but an initial test to this end has been performed. The ZnDPY photosensitizer, 588 µL of 5.29×10^{-4} M in THF, 11.5 mL of 1.88×10^{-4} M FeF20TPPCl in THF, and 4.7 g of phenol were all combined with 11.9 mL of THF in the photoreactor and bubbled for 15 minutes with CO_2. Benzyl mercaptan (1.0 mL of 99%), the electron donor, was injected through a septum attached to the top of the photoreactor, creating a total volume of 25 mL. This was added last as a health and safety precaution. Light from the 300 W Xe Arc lamp set at 275 W from the power supply was set on the reaction mix stirred by a magnet and magnetic stir plate (Barnstead/Termolyne model 846415) for over 24 hours. During this time, 8 sets of 0.9 mL GC samples were taken randomly over the course of 31 hours from a septum on the top of the photoreactor by a gas-tight GC syringe to assess the progress of the reaction.

A final note regarding the reaction apparatus should be made concerning the photoreactor. The photoreactor itself is a specialized flask with a volume of 197.10 ± 0.13 mL. Given that only 25 mL of volume is taken up by the reaction mix, CO has roughly 172 mL of headspace to diffuse through. More CO would have to be produced overall in order to have an amount high enough to be in range of the calibration. Taking a 0.9 mL sample would only encompass a small fraction (0.9/172) of the volume CO occupies, and thus would only represent a small fraction of the total CO produced. These fractions comprise the data that is analyzed.

RESULTS AND DISCUSSION

Reaction Apparatus

Given the results of the flow rate and temperature control experiments, the following apparatus was created for the photosensitizer reaction experiments (Figure 11).

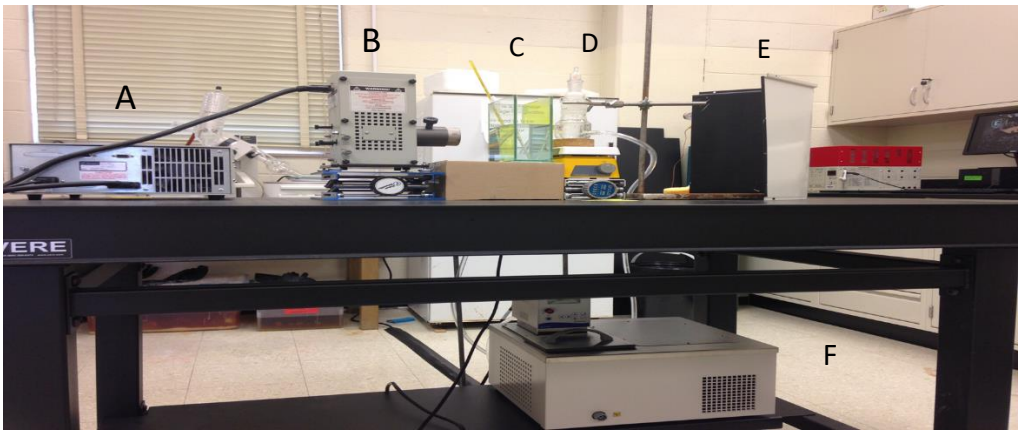

Figure 11. Reaction apparatus, consisting of a power source from Oriel Instruments (A), a 300 W Xe arc lamp (B), a water filter attached to a long pass filter (C), a photoreactor and the magnetic stir plate underneath it (D), a light shield (E), and a circulator (F).

From left to right, the 300 W Xe arc lamp emits light into a water filter attached to a long pass filter, which blocks out light with wavelengths lower than 470 nm. The long pass filter was needed in order to block out light with higher energy than the visible spectra. Figures 12 and 13 represent two replicate experiments without a water filter. As demonstrated by these figures, temperature was not adequately controlled by the jacketed photoreactor, indicating the necessity of the water filter seen in Figure 11.

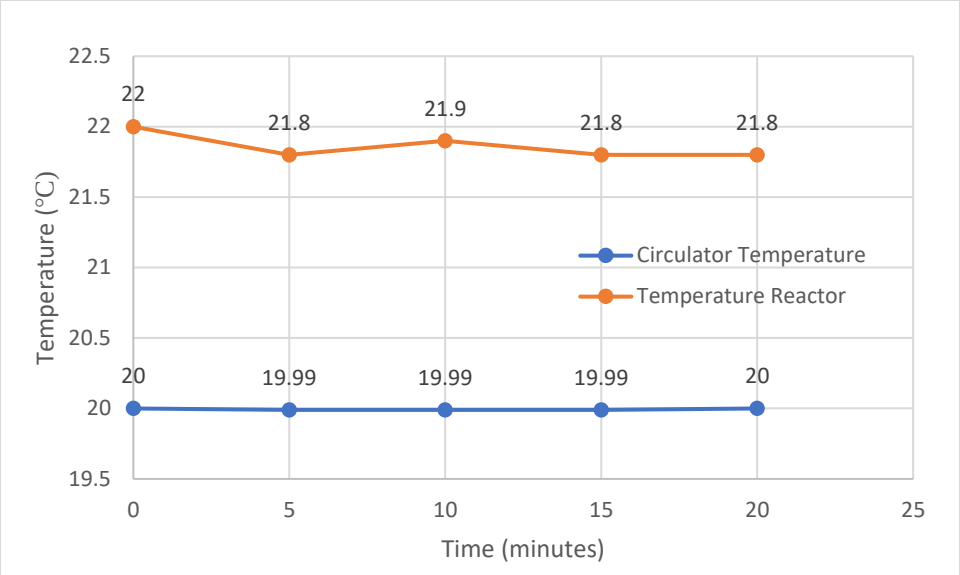

Figure 12. First test on effectiveness of the circulator. The orange line represents temperature in the reactor over time while the blue line represents the temperature of the circulator over time. Each dot represents a measurement.

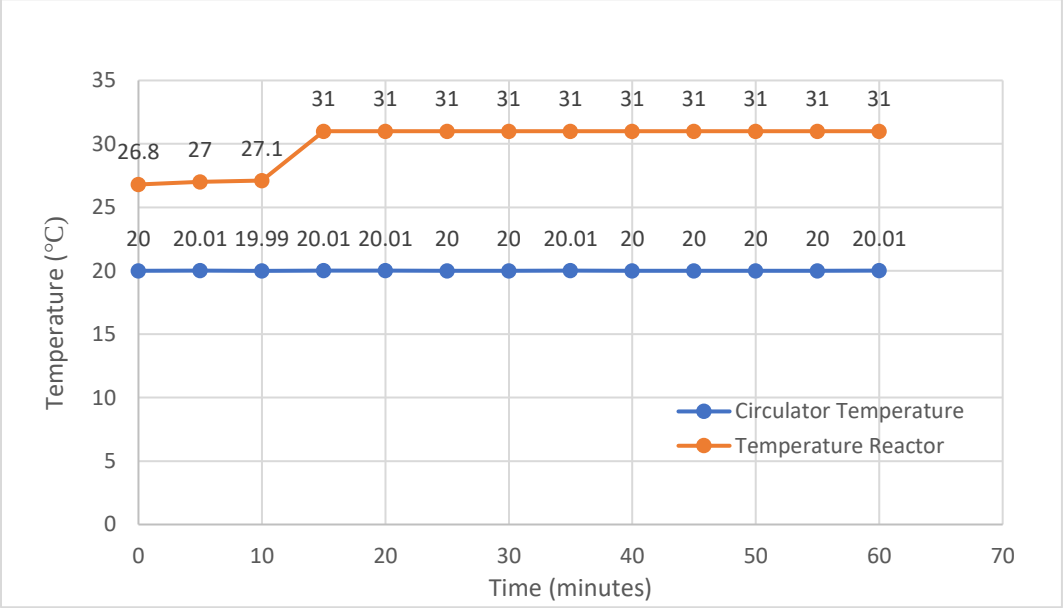

Figure 13. Second test of efficiency of the temperature regulator. The orange line represents temperature in the reactor over time while the blue line represents the temperature of the circulator over time. Each dot represents a measurement.

In both these experiments, light from the 300 W Xe Arc lamp set at 275 W by the power supply was incident on water in the photoreactor without passing through any sort of light filter. The photoreactor was hooked up to the circulator so that it would ideally keep the temperature at set temperature. The temperature of the circulator was measured by the instrument while the temperature in the

photoreactor was measured by a mercury thermometer. While both figures show that the temperature stabilized over time, the issue stems from the circulator being set to the same temperature but stabilizing at two different temperatures between experiments. The point of the circulator was to keep the reaction at a given temperature in order to compare the results to literature. Even if comparing papers that might use "room temperature" as designation, the temperature of the lab varies greatly throughout the year, which creates a variable that needs to be addressed to conduct effective experimentation. While it could keep the temperature stable over time, these experiments showed a lack of control over choosing the temperature of the reactor, resulting in lower reproducibility and comparability.

Next in the apparatus is the photoreactor, which is hooked up to the temperature-controlled water bath via tygon hoses. This was deemed necessary based on pass/fail tests of several different submersible water pumps. Light needs to be able to hit the reaction mix, and setups that would allow light to hit a container in the circulator were ruled out. This would involve actions such as placing lights in the circulator along with the reaction container, which could easily clutter the limited space inside the circulator. Instead, methods were pursued that involved using the instrument's pumping function to transfer the water into something else. Because the instrument did not have a separate intake function to circulate the water back into the instrument, two different fish tank pumps were implemented individually in their own set of experiments to determine if the flow rate could be sustained for long periods of time. No matter the variation of power on either of the pumps, neither could not keep up with the instrument's flow rate for longer than 10 minutes. The photoreactor seen in Figure 14 comes with a water jacket that facilitates constant flow by closing the system and directing the water back into the instrument, allowing the water to be returned to the circulator at a constant rate. This would keep the circulator from getting too empty or too full, which would cause it to turn off.

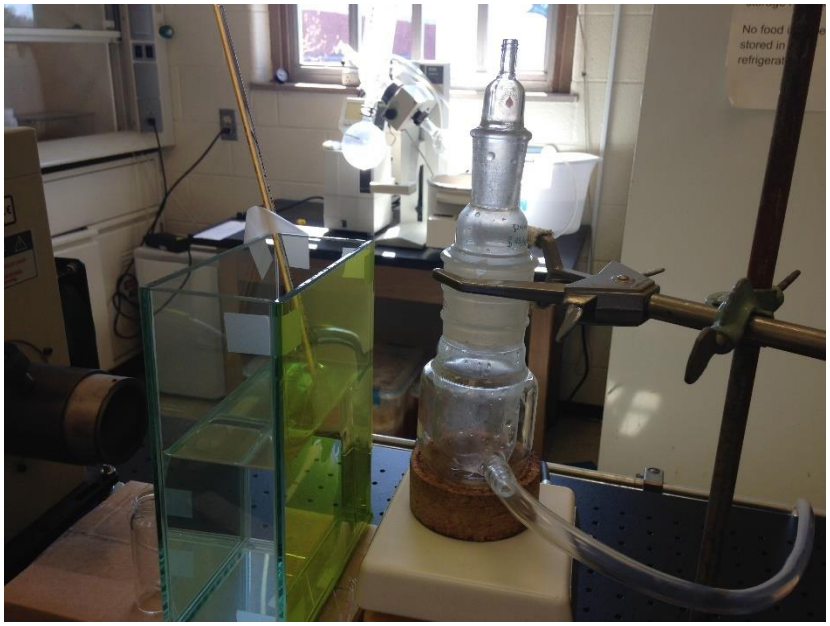

Figure 14. Close up of the water filter and the uncapped photoreactor. It is capped with a septum during runs.

Underneath the photoreactor is a magnetic stir plate which was used to keep the reaction mixture homogenous. Following the photoreactor, a light shield was placed so that light would not continue to be cast past the reactor. Objects such as lab jacks and cork rings were placed and rearranged underneath components as necessary to ensure the alignment of the optical path between the lamp and the reaction mix.

GC Calibration

Calibration gas injections were conducted in order to find the optimal configurations for separating the expected gases from the reaction.

Table 1. Table of GC runs with calibration gas

Trial #	Flow rate mL/min	Oven Temp (°C)	TCD Temp (°C)	Sample volume mL
1	10	50	205	0.5
2	11.7	50	205	0.5
3	13.3	50	205	0.5
4	20	50	205	0.5
5	25	50	205	0.5

6	30	50	205	0.5
7	30	50	205	0.5
8	13.3	70	205	0.5
9	15	70	205	0.5
10	16.7	70	205	0.5
11	20	70	205	0.5
12	25	70	205	0.5
13	10	100	205	0.5
14	15	100	205	0.5
15	20	100	205	0.5
16	30	25	205	0.5
17	20	40	205	0.5
18	16.7	55	205	0.5
19	10	50	205	0.1
20	30	50	205	0.1
21	16.7	60	205	0.5
22	15	60	205	0.5
23	15	60	205	0.5

Optimal parameters are highlighted. Flow rates calculated from a linear proportion, where 6 PSI=10 mL/min.

Table 1 summarizes the parameters for all the different runs. While temperature was directly set, the flow rate required calculation. The flow rate is dependent and proportional to the pressure of the carrier gas, varied in terms of PSI by the instrument. The flow rate was calculated via a relation that was given by the manufacturer (6 PSI= 10 mL/min). Since this relation did not always yield a whole number, some values are approximated to one decimal place. Runs 1-15 tested different flow rates at sets of constant temperatures, ultimately finding that a flow rate of 15 mL/min and a temperature of 70°C produces the narrowest and most distinguishable peaks. Runs 16-18 and 21 were conducted throughout the different temperature runs to determine whether the next set of trials should have increased or decreased temperature. Runs 19 and 20 were conducted to see if injecting a lower volume of gas would be more efficiently separated by the instrument (it made little difference), and runs 22 and 23 and runs 6 and 7 were conducted to test the reproducibility of the runs. These last runs produced the same result. After conducting the trials, selecting the ideal GC parameters was a matter of comparing the graphs to see which produced the narrowest and most distinguishable peaks. For example, comparing

the working parameters of run 9 with run 11, run 9 (Figure 15) was chosen because it produced a more pronounced CO peak than run 11 (Figure 16).

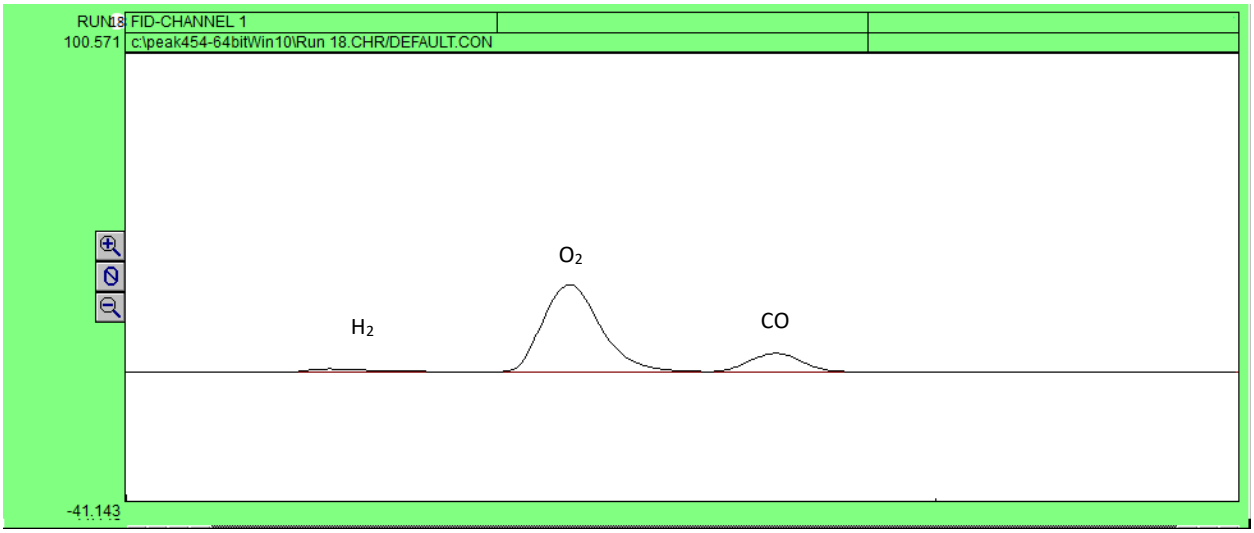

Figure 15. 0.5 mL calibration gas injection with column temp at 70°C and flow rate of 15 mL/min (9 PSI). The peaks are labelled with the gases they represent.

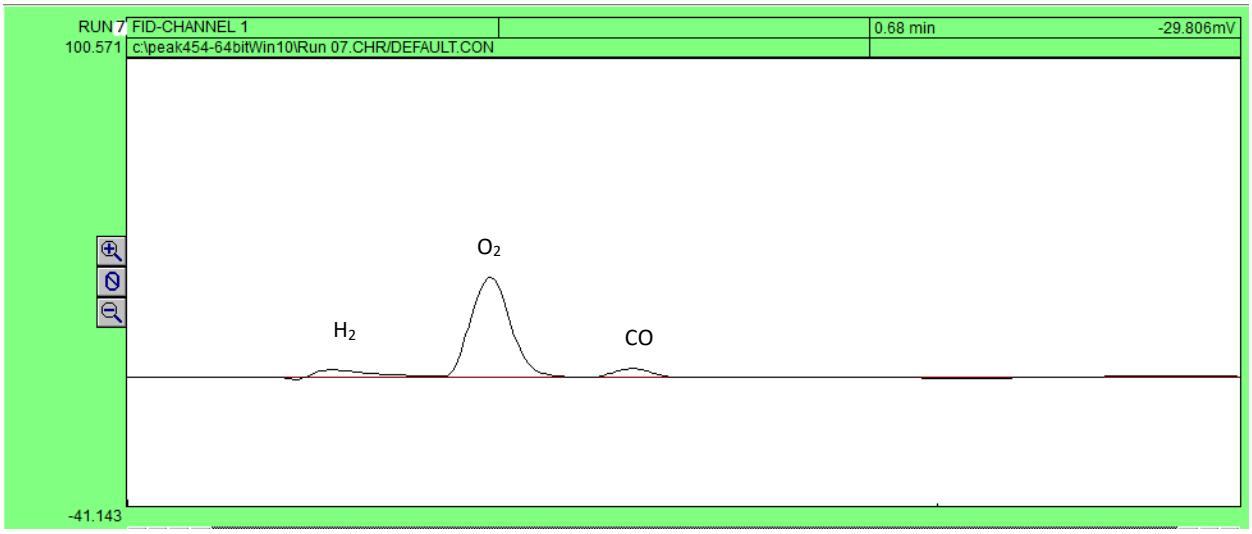

Figure 16. 0.5 mL calibration gas injection with 70°C column temperature and 20 mL/min (12 PSI). The peaks are labelled with the gases they represent.

Each peak was assigned by comparing the order of the peaks to those of a similar experiment conducted by RESTEK, the company that produced the 5 Å molecular sieve column (Figure 17).[36]

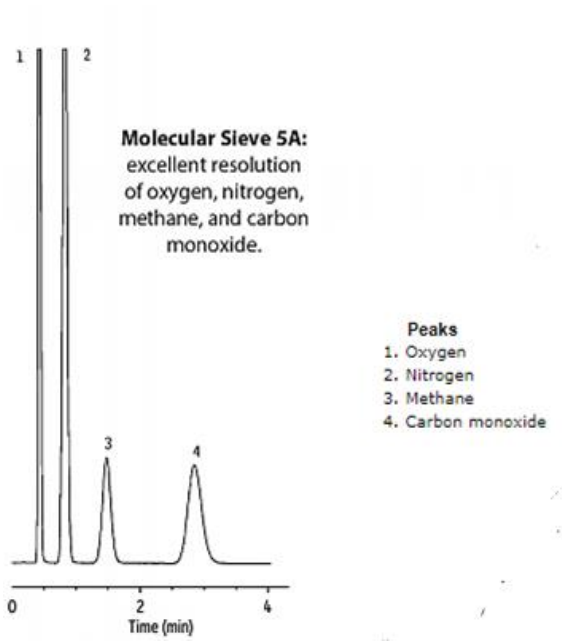

Figure 17. Chromatograph with a 5 Å molecular sieve column with helium as the carrier gas.[36]

Figure 17 shows a chromatograph experiment with a gas mixture of oxygen, nitrogen, methane, and carbon monoxide with helium carrier gas. As Figure 16 shows, there are only 3 peaks detected, which relate to three of the gases in the calibration gas (0.5% by mol CO_2, CO, O_2, and H_2 each in nitrogen). Since nitrogen is the carrier gas in this experiment, that peak would not be observed. Carbon dioxide gets stuck in the column due to its shape and size, so that is likely not to be detected. Methane is not in the calibration gas either, so that peak should not be seen. This leaves oxygen, hydrogen, and carbon monoxide. Given the results of the literature experiment, hydrogen would elute first, oxygen elutes second, and carbon monoxide third. The peaks represent hydrogen, oxygen, and carbon monoxide going from left to right.

Calibration experiments followed in which 9 injections of calibration gas (0.5% by mol CO_2, CO, O_2, and H_2 each in nitrogen) were injected in 0.1 mL increments starting from a 0.1 mL injection an ending in a 0.9 mL injection. The calibration experiments yielded the following graph:

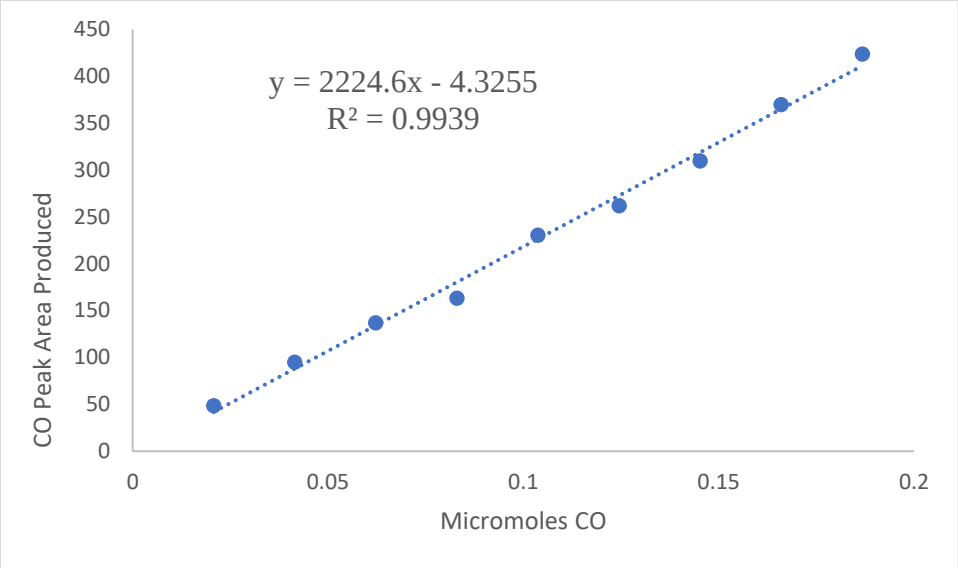

Figure 18. Plot of micromoles of CO vs peak area of the CO peak produced. The dots represent individual injections and the dashed line represents the linear regression line of best fit.

Figure 18 was produced by converting volume of the injected calibration gas to micromoles of CO injected by using the ideal gas equation (Equation 1), with a temperature of 293.65 K measured by digital thermometer. As indicated by the R^2 value, a strong linear correlation was produced from this calibration. The range of calibration was established from 0.1-0.9 mL of calibration gas, which through the ideal gas law equation translates into a range of 0.0208-0.187 micromoles that the detector can linearly correlate to peak area values through the calibration. Accounting for the headspace, the reaction would have to produce 3.98-35.74 micromoles to stay within range of this calibration.

The First CO_2Reduction Photocatalysis Experiment

When 588 µL of 5.28×10^{-4} M ZnDPY photosensitizer in THF, 11.5 mL of 1.88×10^{-4} M iron catalyst, in THF, 4.7 g of phenol mixed with 11.9 mL of THF, and 1 mL of 99% benzyl mercaptan were put into the apparatus and set to run, curious results were obtained—as seen in Figure 19.

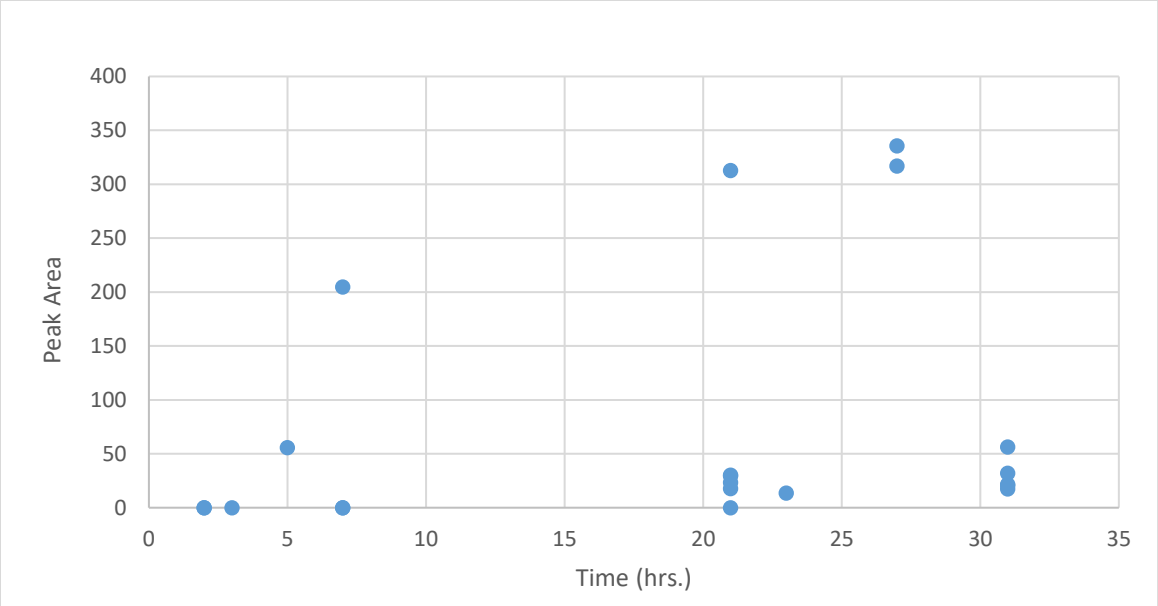

Figure 19. Summary of CO detected at a given time in the reaction. The dots represent the CO peak area produced from an individual injection of a 0.9 mL of sample, except for a point at the 7 hour mark which had 2 separate measurements of 0.

For any given reaction that takes place, one would generally expect there to be an increase in the amount of products over time and plateau as the reaction near completion. Figure 19 shows experimental data for reduction of CO_2 to CO. Multiple times throughout the experiment, CO was detected in varying amounts contrary to this general trend. At hour seven, this odd behavior is exemplified by the results of a 0.9 mL injection indicating an absence of CO followed by results indicating a presence of CO followed by another injection indicating no CO. This occurred among trials that took place roughly 20 minutes between each other. Since this is far from optimal behavior, more work is necessary to create experiments to assess the abilities of ZnDPY as a photosensitizer.

FUTURE WORK

In regards to future work, there is much to be done. The odd behavior exhibited by the first photocatalysis experiments need to be explored. Possible routes would be to change the concentrations of the reaction mix to produce more CO and to further investigate the headspace effects. It is possible that the production of CO was not sufficient enough for the samples to be consistently detected by the GC. The photoreactor was perfused with CO_2 and there was more than enough light to supply photons for the reaction. Assuming the electron donor is the limiting reagent, at the current concentrations, the theoretical yield would be 4,267 micromoles of CO, well above the mark of the calibration. At some point during the reaction, theoretically there should be enough CO to be detected. However, the reaction does not necessarily have to produce the theoretical amount, and even if it does, the sample collected from the headspace may not have enough CO_2 to detect. Another possibility along this line is that THF significantly dissolves CO, further reducing the amount of CO in the headspace. This aspect will need to be explored through future studies.

While the apparatus appears to do its job proficiently, there could be improvements. Besides the issue of the headspace of the photoreactor, the long pass filter that was implemented does take damage from the lamp light and loses its ability to filter higher energy light over time. This would allow higher energy light to hit the reaction mixture, potentially degrading the iron catalyst and the photosensitizer and stopping the reaction. Reaction procedures will need to be made for the other photosensitizers synthesized by the lab, and variables in the reaction, such as temperature and acidity, should be varied to see what trends arise. Lastly, the abilities of ZnDPY still need to be compared to other known photosensitizers, so experiments need to be conducted to find where ZnDPY stands among other photosensitizers.

REFERENCES

1. U.S. Global Change Research Program. Introduction to Our Changing Climate. https://nca2014.globalchange.gov/report/our-changing-climate/introduction (accessed Mar 12, 2019)
2. Climate Central. The 10 Hottest Global Years on Record. https://www.climatecentral.org/gallery/graphics/the-10-hottest-global-years-on-record (accessed Apr 6, 2019).
3. Thomas, C. D.; Cameron, A.; Green, R. E.; Bakkenes, M.; Beaumont, L. J.; Collingham, Y. C.; Erasmus, B. F. N.; Siqueira, M. F. de; Grainger, A.; Hannah, L.; Hughes, L.; Huntley, B.; Jaarsveld, A. S. van; Midgley, G. F.; Miles, L.; Ortega-Huerta, M. A.; Peterson, A. T.; Phillips, O. L.; Williams, S. E. Extinction risk from climate change. *Nature* **2004,** *427*, 145–148.
4. United Nations. Climate Change. http://www.un.org/en/sections/issues-depth/climate-change/index.html (accessed Mar 12, 2019).
5. Krane, J. Climate change and fossil fuel: An examination of risks for the energy industry and producer states**.** *Energy and Sustainability* **2017,** *4***,** E2.
6. Environmental Protection Agency. Global Greenhouse Gas Emissions Data. https://www.epa.gov/ghgemissions/global-greenhouse-gas-emissions-data (accessed Mar 12, 2019).
7. Graham Research Institute on Climate Change and the Environment. To what extent could planting trees help solve climate change? http://www.lse.ac.uk/GranthamInstitute/faqs/to-what-extent-could-planting-trees-help-solve-climate-change/ (accessed Mar 12, 2019).
8. Environmental Protection Agency. Overview of Greenhouse Gases https://www.epa.gov/ghgemissions/overview-greenhouse-gases (accessed Mar 12, 2019).
9. National Geographic. Causes of Global Warming, Explained. https://www.nationalgeographic.com/environment/global-warming/global-warming-causes/
10. Shehzad, N. Tahir, M. Johari, K. Murugesan, T. Hussain, M. A critical review on TiO_2 based photocatalytic CO_2 reduction system: Strategies to improve efficiency. *Journal of CO_2 Utilization.* **2018**, *26*, 98–122.
11. Zhu, S. Wang, D. Photocatalysis: Basic Principles, Diverse Forms of Implementations and Emerging Scientific Opportunities. *Advanced Energy Materials.* **2017,** *7* (23)**,** 1700841-1700865.
12. Hong, J. Zhang, W. Ren, J. Rong, X. Photocatalytic reduction of CO_2: a brief review on product analysis and systematic methods. *Anal. Methods.* **2012**, *5*, 1086-1097.
13. Tamaki, U. Ishitani, O. Supramolecular Photocatalysts for the Reduction of CO_2. *ACS Catal.* **2017**, *7* (5), 3394-3409.
14. Alqahtani, N. Synthesis and Characterization of Zinc(II) Dipyrrin Photosensitizers. Master's Thesis, East Tennessee State University, Johnson City, TN, 2018.
15. Trinh, C. Kirlikovali, K. Das, S. Ener, M. E. Gray, H. B. Djurovich, P. I. Bradforth, S. E. Thompson, M. E. Symmetry-Breaking Charge Transfer of Visible Light Absorbing Systems: Zinc Dipyrrins. *J. Phys. Chem. C*. **2014**, *118*, 21834-21845.
16. Bartynski, A. N. Gruber, M. Das, S. Rangan, S. Mollinger, S. Trinh, C. Bradforth, S. E. Vandewal, K. Salleo, A. Bartynski, R. A. Bruetting, W. Thompson, M. E. Symmetry-Breaking Charge Transfer in a Zinc Chlorodipyrrin Acceptor for High Open Circuit Voltage Organic Photovoltaics. *J. Am. Chem. Soc.* **2015**, *137*, 5397-5405.

17. Sazanovich, I.V. Krimaier, C. Hindin, E. Lianhe, Y. Bocian, D.F. Lindsey, J.S. Holten, D. Structural Control of the Excited-State Dynamics of Bis(dipyrrinato)zinc Complexes: Self-Assembling Chromophores for Light-Harvesting Architectures. *J. Am. Chem. Soc.* **2004**, *126* (9), 2664-2665.
18. Tungulin, D. Leier, J. Carter, A.B. Powell, A.K. Albuquerque, R.Q. Unterreiner, A.N. Bizzarri, C. Chasing BODIPY: Enhancement of Luminescence in Homoleptic Bis(dipyrrinato) ZnII Complexes Utilizing Symmetric and Unsymmetrical Dipyrrins. *Chemistry- A European Journal* **2019**, *25* (15).
19. Tsuchiya, M. Sakamoto, R. Shimada, M. Yamanoi, Y. Hattori, Y. Sugiomoto, K. Nishibori, E. Nishihara, H. Bis(dipyrrinato)zinc(II) Complexes: Emission in the Solid State. *Inorg. Chem*. **2016**, *55* (12), 5732-5734.
20. Baudron, S.A. Luminescent dipyrrin based metal complexes. *Dalton Transactions*, **2013, (**21).
21. Hanson, K. Tamayo, A. Diev, V.V. Whited, M.T. Djurovich, P.I. Thompson, M.E. Efficient Dipyrrin-Centered Phosphorescence at Room Temperature from Bis-Cyclometalated Iridium(III) Dipyrrinato Complexes*. Inorg. Chem*. **2010**, *49* (13), 6077-6084.
22. McLean, T.M. Moody, J.L. Waterland, M.R. Telfer, S.G. Luminescent Rhenium(I)-Dipyrrinato Complexes. *Inorg. Chem*. **2012,** *51* (1), 446-455.
23. Azacarate, I. Costentin, C. Robert, M. Savéant, J.M. Dissection of Electronic Substituent Effects in Multielectron− Multistep Molecular Catalysis. Electrochemical CO2-to-CO Conversion Catalyzed by Iron Porphyrins. *J. Phys. Chem. C,* **2016***, 120,* 28951−28960.
24. Costentin, C. Robert, M. Savéant, J.M. Current Issues in Molecular Catalysis Illustrated by Iron Porphyrins as Catalysts of the CO2-to-CO Electrochemical Conversion. *Acc. Chem. Res.,* **2015**, *48* (12), 2996–3006.
25. Azcarate, I. Costentin, C. Robert, M. Savéant, J.M. Through-Space Charge Interaction Substituent Effects in Molecular Catalysis Leading to the Design of the Most Efficient Catalyst of CO_2-to-CO Electrochemical Conversion. *J. Am. Chem. Soc.*, **2016**, *138* (51), 16639–16644.
26. Bonin, J. Robert, M. Routier, M. Selective and Efficient Photocatalytic CO_2 Reduction to CO Using Visible Light and an Iron-Based Homogeneous Catalyst. *J. Am. Chem. Soc.* **2014**, *136* (48), 16768-16771.
27. Lian, S. Kodaimati, M.S. Dolzhnikov, D.S. Calzada, R. Weiss, E.A. Powering a CO_2 Reduction Catalyst with Visible Light through Multiple Sub-picosecond Electron Transfers from a Quantum Dot. *J. Am. Chem. Soc.* **2017,** *139* (26), 8931-8938.
28. Pellegrin, Y.,Odobel, F. Sacrificial Electron Donor Reagents for Solar Fuel Production. *Comptes Rendus Chimie*, **2017**, *20*, 283-295.
29. Savéant, J.M. Lexa, D. Bhugun, I. Catalysis of the Electrochemical Reduction of Carbon Dioxide by Iron(0) Porphyrins: Synergystic Effect of Weak Brönsted Acids. *J. Am. Chem. Soc.*, **1996**, *118* (7), 1769–1776
30. Sigma Alderich. Carrier Gas Selection for Capillary Gas Chromatography. https://www.sigmaaldrich.com/content/dam/sigma-aldrich/docs/Supelco/General_Information/1/t411126h.pdf (accessed Apr 5, 2019).
31. Agilent Technologies. Converting Helium Carrier Gas GC Methods Nitrogen and Hydrogen. https://www.agilent.com/cs/library/slidepresentation/public/Converting%20Helium%20Carrier%20Gas%20GC%20Methods%20to%20Nitrogen%20and%20Hydrogen.pdf (accessed Apr 5, 2019).
32. Yu, R. Reckhow, D. Gas Chromatography. http://www.ecs.umass.edu/cee/reckhow/courses/772/slides/772l16.pdf (accessed Apr 5, 2019).

33. Sensue, A. Molecular Sieve Packed Columns and Fixed (Permanent) Gas Analysis. ChromaBLOGraphy. https://blog.restek.com/?p=10643 (accessed Mar 12, 2019).
34. Sensue, A. Molecular Sieve 5A & 13X packed columns – Installation / Conditioning / Helpful Hints https://blog.restek.com/?p=10617 (accessed Mar 12, 2019).
35. SRI Instruments. Detectors: Thermal Conductivity Detectors-TCD.
36. RESTEK. Permanent Gases on Molecular Sieve 5 A and Molecular Sieve 13 X. https://www.restek.com/chromatogram/view/GC_PC00166 (accessed Apr 5, 2019).